Structural Engineering and Mechanics, *Vol. 67, No. 4 (2018) 369-383*
DOI: https://doi.org/10.12989/sem.2018.67.4.369

A new plate model for vibration response of advanced composite plates in thermal environment

Ouahiba Taleb[1,2,3], Mohammed Sid Ahmed Houari[*1,3,4], Aicha Bessaim[1,3,4], Abdelouahed Tounsi[4,5,6] and S.R. Mahmoud[7]

[1]*University Mustapha Stambouli of Mascara, Department of Civil Engineering, Mascara, Algeria*
[2]*Laboratoire des Sciences et Techniques de l'Eau, University Mustapha Stambouli of Mascara, Mascara, Algeria*
[3]*Laboratoire des Structures et Matériaux Avancés dans le Génie Civil et Travaux Publics, Université de Sidi Bel Abbes, Faculté de Technologie, Département de Génie Civil, Algeria*
[4]*Material and Hydrology Laboratory, University of Sidi Bel Abbes, Faculty of Technology, Civil Engineering Department, Algeria*
[5]*Civil and Environmental Engineering Department, King Fahd University of Petroleum & Minerals, Dhahran, Saudi Arabia*
[6]*Laboratoire de Modélisation et Simulation Multi-échelle, Département de Physique, Faculté des Sciences Exactes, Département de Physique, Université de Sidi Bel Abbés, Algeria*
[7]*Department of Mathematics, Faculty of Science, King Abdulaziz University, Jeddah, Saudi Arabia*

(Received April 11, 2018, Revised May 30, 2018, Accepted June 1, 2018)

Abstract. In this work, a novel hyperbolic shear deformation theory is developed for free vibration analysis of the simply supported functionally graded plates in thermal environment and the FGM having temperature dependent material properties. This theory has only four unknowns, which is even less than the other shear deformation theories. The theory presented is variationally consistent, without the shear correction factor. The present one has a new displacement field which introduces undetermined integral variables. Equations of motion are obtained by utilizing the Hamilton's principles and solved via Navier's procedure. The convergence and the validation of the proposed theoretical model are performed to demonstrate the efficacy of the model.

Keywords: FG plates; new plate theory; vibration; analytical modeling; thermal environment

1. Introduction

Functionally graded materials (FGMs) have been increasingly used in the various engineering fields, notably in high temperature applications such as thermo-mechanical loadings structures, spacecraft, aircraft and plasma coatings for fusion reactors (Li *et al.* 2008, Kar and Panda 2015a), the considerable advantages offered by functionally graded materials over conventional materials are eliminated the interface problems of conventional composite materials and the stress distribution becomes mitigated. By gradually varying the volume fraction of constituent materials, their material properties exhibit a smooth and continuous change from one surface to another, thus are being capable to withstand intense high temperature gradient while preserve structural integrity (Huang and Shen 2004). FGMs were firstly designed as thermal barrier materials for aerospace structures and fusion reactors where immensely high temperature and large thermal gradient exist (Ebrahimi 2013). Currently, FGMs are explored in wide engineering applications including mechanical, nuclear, and civil engineering. Hence, examining their responses under various types of loading using accurate models of structures (plates, beams and shell) is extremely important. Subsequently, the static, vibration, thermo-mechanical and buckling and post-buckling analyses of laminated composite and functionally graded structures have been performed by many researchers (Houari *et al.* 2013, Ahmed 2014, Kar and Panda 2014, Panda and Mahapatra 2014, Yaghoobi et *al.* 2014, Belabed *et al.* 2014, Behravan Rad 2015, Sofiyev and Kuruoglu 2015, Akbaş 2015, Darilmaz 2015, Darilmaz *et al.* 2015, Ebrahimi and Dashti 2015, Arani *et al.* 2016, Ebrahimi and Habibi 2016, Mahapatra *et al.* 2016a, b, c, Ebrahimi and Jafari 2016, Sahoo *et al.* 2016, Abdelaziz *et al.* 2017, Kolahchi *et al.* 2017a, b, Sofiyev and Osmancelebioglu 2017, Benahmed *et al.* 2017, Menasria *et al.* 2017, El-Haina *et al.* 2018, Kaci *et al.* 2018, Belabed *et al.* 2018, Younsi *et al.* 2018, Karami *et al.* 2018). Various plate theories have been performed to predict and provide more precisely their responses. These plate theories can be divided into three groups namely: classical plate theory (CPT), first-order shear deformation plate theory (FSDT) and higher-order shear deformation plate theory (HSDT). The first group represents the classical (thin plate) also known as the Kirchhoff plate theory (Kirchhoff 1850) assumes a non-compressible plate model and which neglects the transverse shear deformation effect. The first-order shear deformation plate theory (Reissner 1945) surmounts this problem by taking into account this effect and the literature related to this is described in the second group. The third group describes the refined higher-order shear deformation theories which are either based on the three-dimensional approach or the two dimensional approach with a nonlinear variation of high order axial

*Corresponding author
E-mail: houarimsa@yahoo.fr, ms.houari@univ-mascara.dz

ISSN: 1225-4568 (Print), 1598-6217 (Online)

displacement giving parabolic variation of transverse shear strains through the plate thickness (Kant 1993). Therefore, this theory has been increasingly used to predict the behavior of advanced composite material plates by giving the possibility to increase the accuracy of numerical evaluations for moderately thick plates and very thick plates (Kant and Swaminathan 2001, Wu *et al.* 2008). A few researchers have utilized classical plate theory (CPT) to studies vibration and static behavior of thin functionally graded (FG) plates in thermal environment. Woo *et al.* (2006) investigated the nonlinear vibration of FG plates in thermal environments with arbitrary boundary conditions based on CPT hypothesis and Von-Karman assumptions. Allahverdizadeh *et al.* (2008) used semi-analytical approach to investigate non-linear forced and free vibration of circular functionally graded plate in thermal environment. Chakraverty and Pradhan (2014) have utilized the classical plate theory to investigate the free vibration of functionally graded plate in thermal environment under different boundary conditions. Joshi *et al.* (2016) presented an analytical solution for buckling and free vibration analysis of partially cracked thin orthotropic rectangular plates in thermal environment. Cui and Hu (2016) studied the thermal buckling and natural vibration of uniformly heated rectangular thin plates with stick-slip-stop boundaries. Joshi *et al.* (2017) used classical plate theory and the modified couple stress theory to investigate free vibration and buckling of partially cracked isotropic and FGM micro plates in thermal environment. The classical plate theory ignores the transverse shear effects, provides reasonable results for relatively thin plates, and suffices for computing the first few modes of vibrations (Xiao *et al.* 2007). First-order shear deformation theory considers the transverse shear deformation effects and gives acceptable results for thick and thin plates, but requires the use of shear correction coefficients which is hard to find as it depends on the geometries parameters, the loading, material properties and boundary conditions of each problem (Ferreira *et al.* 2009, Abualnour *et al.* 2018). On the basis of the first-order shear deformation plate theory with von Karman assumptions, Praveen and Reddy (1998) conducted the nonlinear transient thermoelastic analysis of functionally graded ceramic-metal plates using finite element formulation under thermal and mechanical loadings. Sundararajan *et al.* (2005) used the first-order shear deformation theory (FSDT) and von- Karman's nonlinearity theory to obtain nonlinear vibration response of functionally graded plate in thermal environment. Alijani *et al.* (2011) provided an analytical solution for the nonlinear free vibration behavior of FG rectangular plates in thermal environments using the FSDT and the von-Karmans nonlinearity. Based on the first order shear deformation theory of shells, the free vibration analysis of rotating functionally graded cylindrical shells with temperature-dependent material properties is presented by Malekzadeh and Heydarpour (2012)**.** Duc and Cong (2015) presented an analytical approach to investigate the nonlinear dynamic response and vibration of (FGM) plates resting on elastic foundation using the first-order shear deformation plate theory. Based on orthotropic Mindlin plate theory. Kolahchi *et al.* (2016a) examined the temperature-dependent nonlinear dynamic stability for a functionally graded CNT reinforced visco-plate resting on an orthotropic elastomeric foundation. Lim and Kim (2017) have presented the micro-mechanical models in thermal environment for the vibration behavior of functionally graded materials plate using first-order shear deformation theory (FSDT). Lei *et al.* (2013) presented the free vibration of FG nanocomposite plates reinforced with single-walled (SWCNTs) in thermal environment, by using first-order shear deformation theory (FSDT) and the element-free kp-Ritz method. The higher-order shear deformation theories (HSDTs) have been developed and do not require any shear correction factor. The HSDT theory predicts more accurate than CPT and FSDT, and it is not necessary to introduce the notion of shear correction factor. Yang and Shen (2002) analyzed free and forced vibration for initially stressed functionally graded plates in thermal environment based on the third-order shear deformation plate theory. Kim (2005) investigated the temperature-dependent vibration of stressed functionally graded rectangular plates using Rayleigh-Ritz procedure. The third-order shear deformation plate theory is adopted to formulate their theoretical model. Free and forced vibration responses of clamped functionally graded plates in thermal environment was investigated by Wattanasakulpong *et al.* (2013) applying the improved third-order shear deformation plate theory of Shi (2007) and Ritz method. Pandey and Pradyumna (2015) have studied the free vibration behaviour of functionally graded sandwich plate using the layerwise finite element formulation with different thermal environment. Parandvar and Farid (2016) studied the dynamic response of functionally graded material (FGM) plates subjected simultaneously to thermal, static, and harmonic loads based on the Reddy plate theory and nonlinear finite element model. Kar and Panda (2015b) presented an analytical approach to investigate the free vibration responses of shear deformable functionally graded single and doubly curved panels under under various types of thermal loading based on higher order shear deformation theory. Mahapatra and Panda (2015) studied the non-linear vibration of the laminated composite curved panel of different geometries under thermal environment based on higher-order shear deformation theory by taking Green-Lagrange type of non-linear kinematics. Mehar *et al.* (2016) computed the natural frequency of the functionally graded carbon nanotube (FG-CNT) composite plate in thermal environment by a finite element formulation based on higher order shear deformation theory. The analysis of nonlinear vibration and dynamic response of functionally graded simply supported plates in thermal environment was studied by Huang and Shen (2004). Hirwani and Panda (2018), also, studied the nonlinear frequency of pre-damaged curved layered composite panel structure using higher-order finite element method including the excess geometrical distortion via Green–Lagrange nonlinearity. Hirwani *et al.* (2018a) developed an analytical procedure for determining the deflection responses of the damaged doubly curved shallow shell panels under the combined thermomechanical loading using two higher-order displacement kinematic theories and solved via finite element method. Within the last two decades, the classic, first order and refined higher-order shear deformation theories had been developed and

improved for functionally graded structures (Li and Cheng 2009, Mahi *et al.* 2015, Malekzadeh and Monajjemzadeh 2016). While a series of two-dimensional and three-dimensional elasticity solutions have been obtained for FGM beams and plates subjected to thermal environment. Li *et al.* (2009) presented free vibration analysis of FGM rectangular plates with simply supported and clamped edges in thermal environment based on three-dimensional elasticity theory and solved with the Ritz method. Lim *et al.* (2009) studied the in-plane vibration of functionally graded circular arches in thermal environment using 2-D theory of elasticity by means of the combination of the Fourier series expansion and the state space method. Malekzadeh *et al.* (2010) analyzed free vibration of thick functionally graded annular plates in thermal environment based on three-dimensional elasticity theory of and differential quadrature method. Setoodeh *et al.* (2012) obtained two-dimensional elasticity solutions for free vibration analysis of elastically supported sandwich beams with functionally graded face sheets subjected to thermal environment using two-dimensional finite element method. We also note that many studies are available on the composite structure solved the frequency, deflection, and dynamic responses either numerical, experimental or via simulation for the of classical and advanced composite structures under the effect of mechanical and/or thermal and hygrothermal loading (Mahapatra *et al.* 2015, Madani *et al.* 2016, Mahapatra and Panda 2016, Mehar *et al.* 2017a, b, Sahoo *et al.* 2017, Hirwani *et al.* 2017, Hadjmohammad *et al.* 2017, Hirwani *et al.* 2018b, c). Recently, Tounsi and his colleagues (Tounsi *et al.* 2016, Houari *et al.* 2016, Hachemi *et al.* 2017, Mouffoki *et al.* 2017) developed a novel refined plate theory for bending, buckling and free vibration of FGM plate and beam with only three unknown functions using various polynomial and non-polynomial functions. Most recently, Tounsi and his co-workers (Khetir *et al.* 2017, Chikh *et al.* 2017) developed another novel refined and robust plate theory for mechanical behaviour of simply supported plate with only four unknown. These theories have a new displacement field which introduces undetermined integral variables. As opposed to five or even greater numbers in the case of other higher shear deformation theories. The most interesting feature of this theory is that it accounts for a parabolic variation of the transverse shear strains across the thickness and satisfies the zero traction boundary conditions on the top and bottom surfaces of the plate without using shear correction factors. The purpose of this paper is to extend the novel refined and robust plate theory developed by Tounsi and his colleagues (Khetir *et al.* 2017, Chikh *et al.* 2017, Besseghier *et al.* 2017) to the free vibration of functionally graded plates in thermal environment. Using the proposed theory, both free vibration analysis of FG plates in thermal environment are investigated. Three types of environmental condition namely uniform, linear and nonlinear thermal load are imposed at the upper and lower surface for simply supported FG plates. The material properties of functionally graded plate are supposed to be temperature-dependent and vary gradually along the thickness direction via power-law model. In this study, analytical of vibration solutions are obtained for functionally graded plate and accuracy is verified by comparing the obtained results with those reported in the literature. The influences of some parameters including gradient index, plate geometry, mode number and thermal loading on the vibration characteristics of the FG plates are presented. It can be concluded that the present theories are not only accurate but also simple in predicting the free vibration responses of temperature-dependent FG plates.

2. Theoretical formulation

2.1 Power-law FG plate equations based

Consider a simply supported rectangular functionally graded plate of length a, width b and uniform thickness h in the unstressed reference configuration. The coordinate system for FG plates is shown in Fig. 1. The FG plate is made of elastic and isotropic functionally graded material with its material properties vary smoothly through the thickness direction only. The effective material properties of the FG plate such as Young's modulus $E(z)$, thermal conductivity $k(z)$, thermal expansion $\alpha(z)$ and mass density $\rho(z)$ based on power function of the volume fractions of the constituents can be expressed as follows

$$P_{eff}(z) = P_m + (P_c - P_m)\left(\frac{z}{h} + \frac{1}{2}\right)^p \tag{1}$$

To predict the behavior of FGMs under high temperature more precisely, it is needful to consider the temperature dependency on material properties. The nonlinear equation of thermo-elastic material properties in function of temperature $T(K)$ can be expressed as the following (Shahrjerdi *et al.* 2011, Attia *et al.* 2015, Kar *et al.* 2017)

$$P(z) = P_0\left(P_{-1}T^{-1} + 1 + P_1T + P_2T^2 + P_3T^3\right) \tag{2}$$

where $P(z)$ denotes material property and $T=T_0+\Delta T(z)$ indicates the environmental temperature; $T_0=300(K)$ is room temperature; P_{-1}, P_0, P_1, P_2 and P_3 are the coefficients of temperature dependent material properties unique to the constituent materials which can be seen in the table of materials properties (Table 1) for FG (ZrO_2/Ti-6Al-4V) and (Si_3N_4/SUS304) (Kim 2005, Shahrjerdi *et al.* 2011, Attia *et al.* 2015), and $\Delta T(z)$ is the temperature rise only through the thickness direction, whereas thermal conductivity k is temperature-independent.

2.2 Constitutive equations

For elastic and isotropic FGMs, the linear constitutive relations can be written as

$$\begin{Bmatrix}\sigma_x\\ \sigma_y\\ \tau_{xy}\end{Bmatrix} = \begin{bmatrix}Q_{11} & Q_{12} & 0\\ Q_{12} & Q_{22} & 0\\ 0 & 0 & Q_{66}\end{bmatrix}\begin{Bmatrix}\varepsilon_x\\ \varepsilon_y\\ \gamma_{xy}\end{Bmatrix} \quad \begin{Bmatrix}\tau_{yz}\\ \tau_{xz}\end{Bmatrix} = \begin{bmatrix}Q_{44} & 0\\ 0 & Q_{55}\end{bmatrix}\begin{Bmatrix}\gamma_{yz}\\ \gamma_{xz}\end{Bmatrix} \tag{3}$$

where (σ_x, σ_y, τ_{xy}, τ_{yz}, τ_{xz}) and (ε_x, ε_y, γ_{xy}, γ_{yz}, γ_{xz}) are the stress and strain components, respectively. Using the material properties defined in Eq. (3), stiffness coefficients, Q_{ij}, can

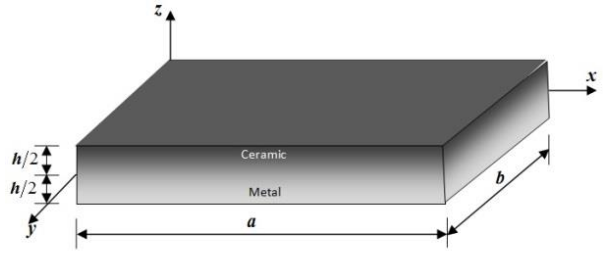

Fig. 1 Geometry of rectangular FGM plate with uniform thickness in the rectangular Cartesian coordinates

be expressed as

$$Q_{11}=Q_{22}=\frac{E(z,T)}{1-\nu^2},\ Q_{12}=\frac{\nu\,E(z,T)}{1-\nu^2},\qquad Q_{44}=Q_{55}=Q_{66}=\frac{E(z,T)}{2(1+\nu)}, \tag{4}$$

Based on the thick plate theory, the basic assumptions for the displacement field of the plate can be described as

$$u(x,y,z,t)=u_0(x,y,t)-z\frac{\partial w_0}{\partial x}+k_1\,f(z)\int\theta(x,y,t)\,dx \tag{5a}$$

$$v(x,y,z,t)=v_0(x,y,t)-z\frac{\partial w_0}{\partial y}+k_2\,f(z)\int\theta(x,y,t)\,dy \tag{5b}$$

$$w(x,y,z,t)=w_0(x,y,t) \tag{5c}$$

The coefficients k_1 and k_2 depends on the geometry and the proposed theory of present study has a hyperbolic function in the form (Nguyen 2015)

$$f(z)=\sinh^{-1}\left(\frac{3z}{h}\right)-z\frac{6}{h\sqrt{13}} \tag{6}$$

It can be observed that the kinematic in Eq. (5) uses only four unknowns (u_0, v_0, w_0 and θ). Nonzero strains of the five variable plate model are expressed as follows

$$\begin{Bmatrix}\varepsilon_x\\ \varepsilon_y\\ \gamma_{xy}\end{Bmatrix}=\begin{Bmatrix}\varepsilon_x^0\\ \varepsilon_y^0\\ \gamma_{xy}^0\end{Bmatrix}+z\begin{Bmatrix}k_x^b\\ k_y^b\\ k_{xy}^b\end{Bmatrix}+f(z)\begin{Bmatrix}k_x^s\\ k_y^s\\ k_{xy}^s\end{Bmatrix},\qquad \begin{Bmatrix}\gamma_{yz}\\ \gamma_{xz}\end{Bmatrix}=g(z)\begin{Bmatrix}\gamma_{yz}^0\\ \gamma_{xz}^0\end{Bmatrix},\quad \varepsilon_z=0 \tag{7}$$

where

$$\begin{Bmatrix}\varepsilon_x^0\\ \varepsilon_y^0\\ \gamma_{xy}^0\end{Bmatrix}=\begin{Bmatrix}\dfrac{\partial u_0}{\partial x}\\ \dfrac{\partial v_0}{\partial x}\\ \dfrac{\partial u_0}{\partial y}+\dfrac{\partial v_0}{\partial x}\end{Bmatrix},\quad \begin{Bmatrix}k_x^b\\ k_y^b\\ k_{xy}^b\end{Bmatrix}=\begin{Bmatrix}-\dfrac{\partial^2 w_0}{\partial x^2}\\ -\dfrac{\partial^2 w_0}{\partial y^2}\\ -2\dfrac{\partial^2 w_0}{\partial x\partial y}\end{Bmatrix},\quad \begin{Bmatrix}k_x^s\\ k_y^s\\ k_{xy}^s\end{Bmatrix}=\begin{Bmatrix}k_1\theta\\ k_2\theta\\ k_1\dfrac{\partial}{\partial y}\int\theta\,dx+k_2\dfrac{\partial}{\partial x}\int\theta\,dy\end{Bmatrix}, \tag{8a}$$

$$\begin{Bmatrix}\gamma_{yz}^0\\ \gamma_{xz}^0\end{Bmatrix}=\begin{Bmatrix}k_2\int\theta\,dy+\dfrac{\partial\varphi_z}{\partial y}\\ k_1\int\theta\,dx+\dfrac{\partial\varphi_z}{\partial x}\end{Bmatrix} \tag{8b}$$

and

$$g(z)=\frac{df(z)}{dz} \tag{8c}$$

It can be observed from Eq. (7) that the transverse shear strains (γ_{xz}, γ_{yz}) are equal to zero at the upper ($z=h/2$) and lower ($z=-h/2$) surfaces of the plate. A shear correction coefficient is, hence, not required. The integrals used in the above equations shall be resolved by a Navier type procedure and can be expressed as follows

$$\frac{\partial}{\partial y}\int\theta\,dx=A'\frac{\partial^2\theta}{\partial x\partial y},\quad \frac{\partial}{\partial x}\int\theta\,dy=B'\frac{\partial^2\theta}{\partial x\partial y},\quad \int\theta\,dx=A'\frac{\partial\theta}{\partial x},\quad \int\theta\,dy=B'\frac{\partial\theta}{\partial y} \tag{9}$$

where the coefficients A' and B' are considered according to the type of solution employed, in this case via Navier method. Therefore, A', B', k_1 and k_2 are expressed as follows

$$A'=-\frac{1}{\alpha^2},\quad B'=-\frac{1}{\beta^2},\quad k_1=\alpha^2,\quad k_2=\beta^2 \tag{10}$$

where α and β are defined in Eq. (32).

2.3 Governing equations

The equations of motion for the free vibration of the FG plate can be derived from the Hamilton's principle

$$\int_{t_1}^{t_2}(\delta K-\delta U)dt=0 \tag{11}$$

where t is the time, t_1 and t_2 are the initial and end times, respectively, δK is the variation of the kinetic energy and δU is the variation of the total strain energy. The total strain energy of the beam can be represented as

$$U=U_d+U_T \tag{12}$$

where U_d is the strain energy due to the mechanical stresses and U_T is the strain energy caused by the initial stresses due to temperature rise. The strain energy U_d and U_T are given by (Shahrjerdi et *al.* 2011, Li et *al.* 2009, Kim 2005)

$$U_d=\frac{1}{2}\int_V\left[\sigma_x\,\varepsilon_x+\sigma_y\,\varepsilon_y+\sigma_z\,\varepsilon_z+\tau_{xy}\,\gamma_{xy}+\tau_{yz}\,\gamma_{yz}+\tau_{xz}\,\gamma_{xz}\right]dV \tag{13}$$

$$U_T=\frac{1}{2}\int_V\left[\sigma_x^T\,d_{11}+\sigma_y^T\,d_{22}\right]dV \tag{14}$$

where d_{ij}, (i, j=1,2) is the nonlinear strain-displacement relationship (Shahrjerdi *et al.* 2011). By substituting d_{ij} into Eq. (14) the following equation is obtained

$$U_T = \frac{1}{2}\int_V \left[\begin{array}{l} \sigma_x^T \left[\left(\dfrac{\partial^2 u}{\partial x^2} + \dfrac{\partial^2 v}{\partial x^2} + \dfrac{\partial^2 w}{\partial x^2} \right) \right] \\ + \sigma_y^T \left[\left(\dfrac{\partial^2 u}{\partial y^2} + \dfrac{\partial^2 v}{\partial y^2} + \dfrac{\partial^2 w}{\partial y^2} \right) \right] \end{array} \right] dV \tag{15}$$

In Eq. (15), the thermal stresses σ_x^T and σ_y^T are given by,

$$\begin{array}{c} \sigma_x^T = -(C_{11}+C_{12})\alpha(z,T)\Delta T(z) \text{ and} \\ \sigma_y^T = -(C_{21}+C_{22})\alpha(z,T)\Delta T(z) \end{array} \tag{16}$$

The kinetic energy of plate can be expressed as

$$K = \frac{1}{2}\int_V \rho(z,T)(\dot{u}+\dot{v}+\dot{w})dV \tag{17}$$

By substituting Eqs. (12)-(17), into Eq. (11) and integrating by parts with respect to space and time variables, the equations of motion in terms of the displacement components of the FG plate are obtained as

$$\begin{array}{l} \left(A_{11}+A_{11}^T\right)d_{11}u_0 + \left(A_{66}+A_{22}^T\right)d_{22}u_0 + (A_{12}+A_{66})d_{12}v_0 \\ -\left(B_{11}+B_{11}^T\right)d_{111}w_0 - \left(B_{12}+2B_{66}+B_{22}^T\right)d_{122}w_0 \\ +\left(B_{66}^s\left(k_1A^{'}+k_2B^{'}\right)+B_{12}^s k_2 B^{'}+B_{22}^{sT}k_1A^{'}\right)d_{122}\theta \\ +\left(B_{11}^s+B_{11}^{sT}\right)k_1A^{'}d_{111}\theta = I_0\ddot{u}_0 - I_1 d_1\ddot{w}_0 + k_1A^{'}J_1 d_1\ddot{\theta}, \end{array} \tag{18a}$$

$$\begin{array}{l} \left(A_{22}+A_{22}^T\right)d_{22}v_0 + \left(A_{66}+A_{11}^T\right)d_{11}v_0 + (A_{12}+A_{66})\,d_{12}u_0 \\ -\left(B_{22}+B_{22}^T\right)d_{222}w_0 - \left(B_{12}+2B_{66}+B_{11}^T\right)d_{112}w_0 \\ +\left(B_{66}^s\left(k_1A^{'}+k_2B^{'}\right)+B_{12}^s k_1A^{'}+B_{11}^{sT}k_2B^{'}\right)d_{112}\theta \\ +\left(B_{22}^s+B_{22}^{sT}\right)k_2B^{'}d_{222}\theta = I_0\ddot{v}_0 - I_1 d_2\ddot{w}_0 + k_2B^{'}J_1\,d_2\ddot{\theta}, \end{array} \tag{18b}$$

$$\begin{array}{l} \left(B_{11}+B_{11}^T\right)d_{111}u_0 + \left(B_{12}+2B_{66}+B_{22}^T\right)d_{122}u_0 \\ +\left(B_{12}+2B_{66}+B_{11}^T\right)d_{112}v_0 + \left(B_{22}+B_{22}^T\right)d_{222}v_0 \\ -\left(D_{11}+D_{11}^T\right)d_{1111}w_0 - 2\left(D_{12}+2D_{66}\right)d_{1122}w_0 \\ -\left(D_{22}+D_{22}^T\right)d_{2222}w_0 + \left(D_{11}^s+D_{11}^{sT}\right)k_1A^{'}d_{1111}\theta \\ +\left(\left(D_{12}^s+2D_{66}^s\right)\left(k_1A^{'}+k_2B^{'}\right)\right)d_{1122}\theta \\ +\left(D_{22}^s+D_{22}^{sT}\right)k_2B^{'}d_{2222}\theta + \left(D_{11}^{sT}k_2B^{'}+D_{22}^{sT}k_1A^{'}\right)d_{1122}\theta \\ -\left(D_{11}^T+D_{22}^T\right)d_{1122}w_0 + A_{11}^T d_{11}w_0 + A_{22}^T d_{11}w_0 = I_0\ddot{w}_0 \\ +I_1\left(d_1\ddot{u}_0+d_2\ddot{v}_0\right) - I_2\left(d_{11}\ddot{w}_0+d_{22}\ddot{w}_0\right) \\ +J_2\left(k_1A^{'}d_{11}\ddot{\theta}+k_2B^{'}d_{22}\ddot{\theta}\right) \end{array} \tag{18c}$$

$$\begin{array}{l} -\left(B_{11}^s+B_{11}^{sT}\right)k_1A^{'}d_{111}u_0 \\ -\left(B_{12}^s k_2B^{'}+B_{22}^{sT}k_1A^{'}+B_{66}^s\left(k_1A^{'}+k_2B^{'}\right)\right)d_{122}u_0 \\ -\left(B_{12}^s k_1A^{'}+B_{11}^{sT}k_2B^{'}+B_{66}^s\left(k_1A^{'}+k_2B^{'}\right)\right)d_{112}v_0 \\ -\left(B_{22}^s+B_{22}^{sT}\right)k_2B^{'}d_{222}v_0 - \left(D_{11}^s+D_{11}^{sT}\right)k_1A^{'}d_{1111}w_0 \\ +\left(\left(D_{12}^s+2D_{66}^s\right)\left(k_1A^{'}+k_2B^{'}\right)\right)d_{1122}w_0 \\ +\left(D_{22}^s+D_{22}^{sT}\right)k_2B^{'}d_{2222}w_0 \\ -\left(H_{11}^s+H_{11}^{sT}\right)\left(k_1A^{'}\right)^2 d_{1111}\theta - \left(H_{22}^s+H_{22}^{sT}\right)\left(k_2B^{'}\right)^2 d_{2222}\theta \\ -\left(2H_{12}^s k_1k_2A^{'}B^{'}+\left(k_1A^{'}+k_2B^{'}\right)^2 H_{66}^s\right)d_{1122}\theta \\ +A_{44}^s\left(k_2B^{'}\right)^2 d_{22}\theta + A_{55}^s\left(k_1A^{'}\right)^2 d_{11}\theta \\ +\left(D_{11}^{sT}k_2B^{'}+D_{22}^{sT}k_1A^{'}\right)d_{1122}w_0 \\ -\left(H_{11}^{sT}\left(k_2B^{'}\right)^2 + H_{22}^{sT}\left(k_1A^{'}\right)^2\right)d_{1122}\theta = \\ -J_1\left(k_1A^{'}d_1\ddot{u}_0 + k_2B^{'}d_2\ddot{v}_0\right) \\ +J_2\left(k_1A^{'}d_{11}\ddot{w}_0 + k_2B^{'}d_{22}\ddot{w}_0\right) \\ -K_2\left(\left(k_1A^{'}\right)^2 d_{11}\ddot{\theta} + \left(k_2B^{'}\right)^2 d_{22}\ddot{\theta}\right) \end{array} \tag{18d}$$

where d_{ij}, d_{ijl} and d_{ijlm} are the following differential operators

$$\begin{array}{c} d_{ij} = \dfrac{\partial^2}{\partial x_i \partial x_j}, \quad d_{ijl} = \dfrac{\partial^3}{\partial x_i \partial x_j \partial x_l}, \\ d_{ijlm} = \dfrac{\partial^4}{\partial x_i \partial x_j \partial x_l \partial x_m}, \quad d_i = \dfrac{\partial}{\partial x_i}, \quad (i,j,l,m=1,2). \end{array} \tag{19}$$

and stiffness components are calculated as

$$\begin{array}{l} \left\{ \begin{array}{l} A_{11}, B_{11}, D_{11}, B_{11}^s, D_{11}^s, H_{11}^s \\ A_{12}, B_{12}, D_{12}, B_{12}^s, D_{12}^s, H_{12}^s \\ A_{66}, B_{66}, D_{66}, B_{66}^s, D_{66}^s, H_{66}^s \end{array} \right\} = \\ \int_{-h/2}^{h/2} C_{11}\left(1, z, z^2, f(z), z\,f(z), f^2(z)\right)\left\{ \begin{array}{c} 1 \\ \nu \\ \dfrac{1-\nu}{2} \end{array} \right\} dz \end{array} \tag{20}$$

$$\begin{array}{l} \left(A_{22}, B_{22}, D_{22}, B_{22}^s, D_{22}^s, H_{22}^s\right) = \\ \qquad \left(A_{11}, B_{11}, D_{11}, B_{11}^s, D_{11}^s, H_{11}^s\right) \end{array} \tag{21}$$

$$A_{44}^s = A_{55}^s \int_{-h/2}^{h/2} C_{44}\left[g^2(z)\right]dz \tag{22}$$

$$\begin{array}{l} \left\{ \begin{array}{l} A_{11}^T, B_{11}^T, D_{11}^T, B_{11}^{sT}, D_{11}^{sT}, H_{11}^{sT} \\ A_{22}^T, B_{22}^T, D_{22}^T, B_{22}^{sT}, D_{22}^{sT}, H_{22}^{sT} \end{array} \right\} = \\ \qquad \int_{-h/2}^{h/2} \left(1, z, z^2, f(z), z\,f(z), f^2(z)\right)\left\{ \begin{array}{c} \sigma_x^T \\ \sigma_y^T \end{array} \right\} dz \end{array} \tag{23}$$

The inertias are also defined as

$$\begin{array}{l} \left(I_0, I_1, J_1, I_2, J_2, K_2\right) = \\ \qquad \int_{-h/2}^{h/2} \left(1, z, f(z), z^2, z\,f(z), f^2(z)\right)\rho(z)dz \end{array} \tag{24}$$

2.4 Temperature field

In this study, four cases of one-dimensional temperature distribution through the thickness are considered, with $T=T(z)$.

2.4.1 Uniform temperature

In this case, a uniform temperature field is used as follows

$$T(z) = T_0 + \Delta T(z) \tag{25}$$

where $\Delta T(z)$ denotes the temperature change and T_0=300K is room temperature.

2.4.2 Linear temperature

For a functionally graded plate, assuming temperatures T_b and T_t are imposed at the bottom and top of the plate, the

temperature field under linear temperature rise along the thickness can be obtained as follows

$$T(z)=T_0+\Delta T\left(\frac{z}{h}+\frac{1}{2}\right) \tag{26}$$

2.4.3 Nonlinear temperature

The nonlinear temperature rise across the thickness of the plate is determined by solving the one dimensional heat conduction equation. The one dimensional steady-state heat conduction equation in the *z*-direction is given by

$$T(z)=-\frac{d}{dz}\left(k(z)\frac{dT}{dz}\right) \tag{27}$$

with the boundary condition $T(h/2)=T_t$ and $T(-h/2)=T_b=T_0$. Here a stress-free state is assumed to exist at $T_0=300K$. The thermal conductivity coefficient $k(z)$ is assumed here to obey the power-law relation in Eq. (5). The analytical solution to Eq. (27) is

$$T(z)=T_b-(T_t-T_b)\frac{\int_{-h/2}^{z}\frac{1}{k(z)}dz}{\int_{-h/2}^{h/2}\frac{1}{k(z)}dz} \tag{28}$$

In the case of power-law FG plate, the solution of Eq. (27) also can be expressed by means of a polynomial series (Shahrjerdi *et al*. 2011, Attia *et al*. 2015, Mahapatra *et al*. 2017)

$$T(z)=T_b+\frac{(T_t-T_b)}{C_{tb}}\left[\left(\frac{2z+h}{2h}\right)-\frac{k_{tb}}{(p+1)k_b}\left(\frac{2z+h}{2h}\right)^{p+1}+\frac{k_{tb}^2}{(2p+1)k_b^2}\left(\frac{2z+h}{2h}\right)^{2p+1}\right.$$
$$\left.-\frac{k_{tb}^3}{(4p+1)k_b^3}\left(\frac{2z+h}{2h}\right)^{3p+1}+\frac{k_{tb}^4}{(4p+1)k_b^4}\left(\frac{2z+h}{2h}\right)^{4p+1}-\frac{k_{tb}^5}{(5p+1)k_b^5}\left(\frac{2z+h}{2h}\right)^{5p+1}\right] \tag{29}$$

with

$$C_{tb}=1-\frac{k_{tb}}{(p+1)k_b}+\frac{k_{tb}^2}{(2p+1)k_b^2}+\frac{k_{tb}^3}{(3p+1)k_b^3}+\frac{k_{tb}^4}{(4p+1)k_b^4}+\frac{k_{tb}^5}{(5p+1)k_b^5} \tag{30}$$

where $kt_b=k_t-k_b$, with k_t and k_b are the thermal conductivity of the top and bottom faces of the plate, respectively.

3. Analytical solution of simply supported FG plate

In this work, we are concerned with the exact solutions of Eq. (20) for a simply supported nanoplate. Using the Navier solution procedure, the following expressions of displacements (u_0, v_0, w_0, and θ) are taken

$$\begin{Bmatrix}u_0\\v_0\\w_0\\\theta\end{Bmatrix}=\sum_{m=1}^{\infty}\sum_{n=1}^{\infty}\begin{Bmatrix}U_{mn}\,e^{i\omega t}\cos(\alpha x)\sin(\beta y)\\V_{mn}\,e^{i\omega t}\sin(\alpha x)\cos(\beta y)\\W_{mn}\,e^{i\omega t}\sin(\alpha x)\sin(\beta y)\\X_{mn}\,e^{i\omega t}\sin(\alpha x)\sin(\beta y)\end{Bmatrix} \tag{31}$$

$$\alpha=m\pi/a\ ,\quad \beta=n\pi/b \tag{32}$$

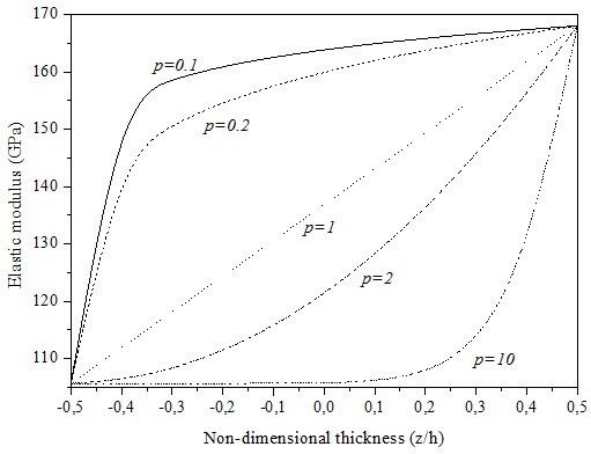

Fig. 2 Variation of elastic modulus versus non-dimensional thickness of FG plate in room temperature field and different values of grading index (p)

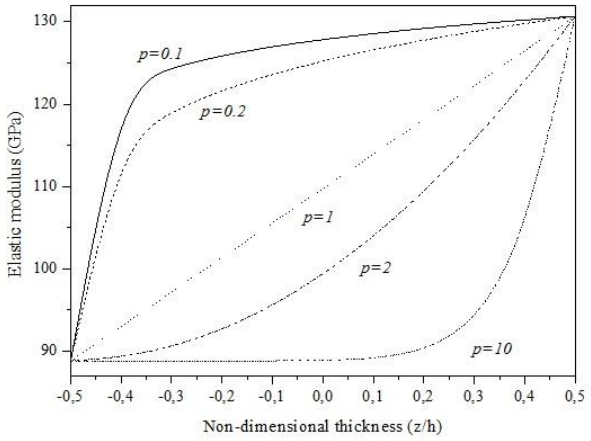

Fig. 3 Variation of elastic modulus versus non-dimensional thickness of FG plate in linear temperature field and different values of grading index (p)

where $i=\sqrt{-1}$, $\alpha=m\pi/a$, β=nπ/b, ω is the natural frequency, and (U_{mn}, V_{mn}, W_{mn}, X_{mn}) are the unknown maximum displacement coefficients.

Substituting Eqs. (31) into Eq. (18), the analytical solutions can be determined by

$$\left(\begin{bmatrix}a_{11}&a_{12}&a_{13}&a_{14}\\a_{12}&a_{22}&a_{23}&a_{24}\\a_{13}&a_{23}&a_{33}&a_{34}\\a_{14}&a_{24}&a_{34}&a_{44}\end{bmatrix}-\omega^2\begin{bmatrix}M_{11}&0&M_{13}&M_{14}\\0&M_{22}&M_{23}&M_{24}\\M_{13}&M_{23}&M_{33}&M_{34}\\M_{14}&M_{24}&M_{34}&M_{44}\end{bmatrix}\right)\begin{Bmatrix}U_{mn}\\V_{mn}\\W_{mn}\\X_{mn}\end{Bmatrix}=\begin{Bmatrix}0\\0\\0\\0\end{Bmatrix} \tag{33}$$

where a_{ij} and M_{ij} are given in Appendix.

4. Results and discussions

4.1 Thermal environment, temperature distributions and material properties

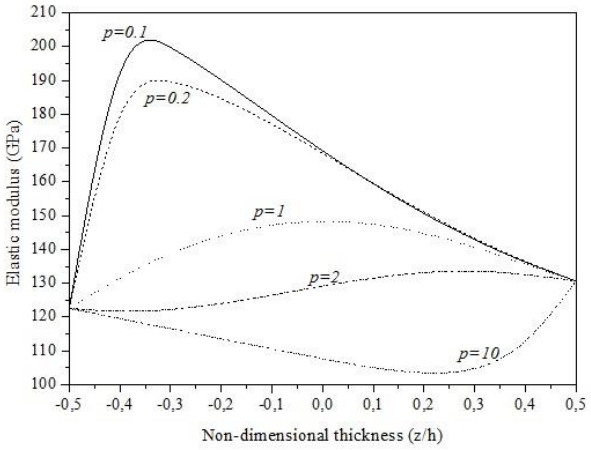

Fig. 4 Variation of elastic modulus versus non-dimensional thickness of FG plate in nonlinear temperature field and different values of grading index (p)

According to the above literature, temperature distribution has a significant influence on the behavior of the FGM plate. Thermal and mechanical properties of the FGMs subjected to high perform surgering temperature have importantly been affected by the temperature variation. For example, Young's modulus of stainless steel, nickel, Ti-6Al-4V, and zirconia is reduced by 37%, 21%, 34% and 31%, respectively, when the temperature rises from room temperature 300−1000(K) (Yang and Shen 2003).

The real structural response of functionally graded plate required to account the temperature dependency of the material properties and temperature distribution through the thickness of the plate. The variation of Young modulus in FG plates through the thickness in room temperature, uniform, linear and nonlinear thermal conditions is presented in Figs. 2-4, respectively. Room temperature is defined at T_0=300(K) for all thermal conditions. The temperature rise in linear temperature is T_b=T_t=600(K), the nonlinear thermal conditions are T_b=0(K) and T_t=600(K) and the sinusoidal thermal conditions are T_b=300(K) and T_t=300(K).

Figs. 2 and 3 show that the variation of elastic Young's modulus of functionally graded plates on room temperature and linear temperature variation with the volume fraction index. It is seen from the above figures that Young's modulus is similar for conditions with room temperature and uniform temperature, but the graphs move to smaller values with the uniform temperature rise. It is clear that Young's modulus decreases with increasing the power law index.

In addition, it can be observed from Fig. 4 that the behavior of Young's modulus in nonlinear thermal loads is completely different from that in room and linear temperature cases. The value of Young's modulus increases close to the lower surface, then decreases when p<1, and the modulus decreases when 1≤p<10. However, Young's modulus decreases then increases close to upper surface for the large value of grading index p>10. Thus, it can be concluded that the environmental conditions type has a considerable effect on Young's modulus.

Table 1 Number of elements used to achieve optimum mesh for isotropic rectangular plates "S4R"

Approximate Global Size	Number of Mesh	$\hat{\omega}_{11}=\omega_{11}h\sqrt{\rho/G}$
$1\times\sqrt{2}$	10×10	0.069079
$0.5\times\sqrt{2}/2$	20×20	0.068438
$0.25\times\sqrt{2}/4$	40×40	0.068266
$0.1\times\sqrt{2}/10$	100×100	0.068218
$0.05\times\sqrt{2}/20$	200×200	0.0682101

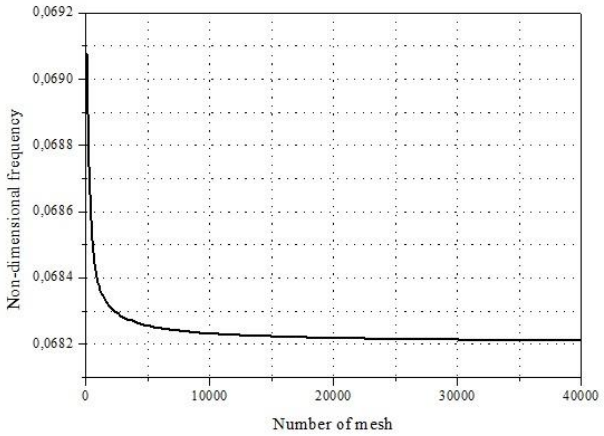

Fig. 5 Mesh Convergence "S4R"

Table 2 Natural frequencies $\hat{\omega}=\omega h\sqrt{\rho/G}$ of an isotropic rectangular plate with v=0.3, a/h=10 and $b=\sqrt{2}a$

(m,n)	Present	(Reddy 1984) (TSDT)	Srinivas *et al.* (1970) 3-D	Abaqus Shell
(1,1)	0.0704	0.0704	0.0704	0.06822
(1,2)	0.1374	0.1374	0.1376	0.1333
(2,1)	0.2015	0.2041	0.2018	0.1988
(2,2)	0.2630	0.2628	0.2634	0.2554

4.2 Validation of the results

4.2.1 Validation

In this section, the accuracy of the presented refined hyperbolic plate theory (RSDT) having with four unknowns only for the free vibration of simply supported isotropic rectangular plates is compared by the analytical solution with those of other available results in the literature and via finite element model using Abaqus software package. In addition, the temperature-dependent FG plates is also demonstrated by comparing the present solution with those of other available results in the literature of higher-order shear deformation theories (Shahrjerdi *et al.* 2011, Huang and Shen 2004) with more unknowns. Thus, the influences various parameters like power law index parameter p, shear deformation, temperature distribution on vibration response of functionally graded plate have been investigated. The non-dimensional frequency parameter is taken as, where

Table 3 Temperature-dependent material properties for (ZrO_2/Ti-6Al-4V) and (Si_3N_4/SUS304)

Material	Properties	P_0	P_{-1}	P_1	P_2	P_3
Si_3N_4	E(GPa)	348.43	0	-3.070×10^{-4}	2.160×10^{-7}	-8.946×10^{-11}
	α(K^{-1})	5.8723×10^{-6}	0	9.095×10^{-6}	0	0
	ρ(Kg/m^3)	2370	0	0	0	0
	v	0.24	0	0	0	0
	k	9.19	0	0	0	0
SUS304	E(GPa)	201.04	0	3.079×10^{-4}	-6.534×10^{-7}	0
	α(K^{-1})	12.330×10^{-6}	0	8.086×10^{-4}	0	0
	ρ(Kg/m^3)	8166	0	0	0	0
	v	0.3262	0	-2.002×10^{-4}	3.797×10^{-7}	0
	k	12.04	0	0	0	0
ZrO_2	E(GPa)	$244.27\times10^{+9}$	0	-1.371×10^{-3}	1.214×10^{-6}	-3.681×10^{-10}
	α(K^{-1})	12.766×10^{-6}	0	-1.491×10^{-3}	1.006×10^{-5}	-6.788×10^{-11}
	ρ(Kg/m^3)	3000	0	0	0	0
	v	0.3330	0	0	0	0
	k	1.80	0	0	0	0
Ti-6Al-4V	E(GPa)	$122.56\times10^{+9}$	0	-4.586×10^{-4}	0	0
	α(K^{-1})	7.75788×10^{-6}	0	6.638×10^{-4}	-3.147×10^{-6}	0
	ρ(Kg/m^3)	4429	0	0	0	0
	v	0.2888	0	1.108×10^{-4}	0	0
	k	7.82	0	0	0	0

Table 4 Non-dimensional natural frequency parameter of simply supported (ZrO_2/Ti-6Al-4V) FG plate in thermal environments

Mode (1,1) Natural frequency of (ZrO_2/Ti-6Al-4V) FG plate		T_b=300(K)				
			T_t=400(K)		T_t=600(K)	
		T_t=300(K)	Temperature-dependent	Temperature-independent	Temperature-dependent	Temperature-independent
ZrO_2	SSDT(a)	8.333	7.614	7.892	5.469	6.924
	TSDT(b)	8.273	7.886	8.122	6.685	7.686
	Present	8.288	7.818	8.070	6.547	7.613
p=0.5	SSDT(a)	7.156	6.651	6.844	5.255	6.175
	TSDT(b)	7.139	6.876	7.154	6.123	6.776
	Present	7.120	6.791	6.968	5.941	6.656
p=1	SSDT(a)	6.700	6.281	6.446	5.167	5.904
	TSDT(b)	6.657	6.435	6.592	5.819	6.362
	Present	6.665	6.383	6.537	5.675	6.275
p=2	SSDT(a)	6.333	5.992	6.131	5.139	5.711
	TSDT(b)	6.286	6.101	6.238	5.612	6.056
	Present	6.294	6.055	6.189	5.476	5.974
Ti-6Al-4V	SSDT(a)	5.439	5.103	5.333	4.836	5.115
	TSDT(b)	5.400	5.322	5.389	5.118	5.284
	Present	5.410	5.290	5.357	5.097	5.250

[a] Shahrjerdi *et al*. (2011) [b] Huang and Shen (2004)

And is at (Shahrjerdi *et al.* 2011, Huang and Shen 2004). Two types of FGMs are considered: (ZrO_2/Ti-6Al-4V) and (Si_3N_4/SUS304). The description of material properties used in the analysis is listed in Table 3.

Example 1

As a first example, the validation of the solution of the proposed refined hyperbolic plate model is carried out by comparing the obtained results with those computed via finite element model using Abaqus software package with considering the mesh convergence study to optimize the results. The FEM solution of Abaqus Software is obtained by using "S4R" shell elements. The analysis of a FEM using Abaqus software package was performed and results were obtained as shown in Table 1 and plotted in Fig. 5. The following parameters are used for numerical computations: $a=10\,h, b=\sqrt{2}\,a, E=1, \nu=0.3, \rho=1$. As clearly shown in Table 1 and Fig. 5, the convergence begins from 10×10 mesh number with lowest non-dimensional frequency 0.069079 and fully converges at 200×200 with lowest non-dimensional frequency 0.0682101, but 100×100 mesh number with lowest non-dimensional frequency 0.068218 was chosen for the comparison, in order to reduce the number of nodes and elements in the analyses.

The present non-dimensional natural frequency parameters $\bar{\omega}=\omega h\sqrt{\rho/G}$ are compared with the different vibration modes using finite element model using Abaqus software, the exact solutions of the three-dimensional elasticity theory (Srinivas *et al.* 1970) and the third shear deformation plates theory (Reddy 1984) for isotropic rectangular plates. For the modes (m, n), the integers m and n denote the number of half-waves in the *x* and *y* directions, respectively. The comparison of the dimensionless frequencies of isotropic square plates for four different planar half-wave numbers (i.e., m and n) are presented in Table 2.

From the examination of Table 2, it is observed that the present refined hyperbolic plate theory (RSDT) yields excellent values of frequencies for all modes of vibration as compared to those of exact solutions of the three-dimensional elasticity theory (Srinivas *et al.* 1970), the third shear deformation plates theory (Reddy 1984) and with the finite element results using Abaqus software package.

Example 2

In this second example, a comparison of the first non-dimensional natural frequency parameters is realized for a (ZrO_2/Ti-6Al-4V) FG plate in thermal environments and the dimensionless fundamental frequencies are tabulated in Table 4.

The FG plate is made of titanium alloy (Ti-6Al-4V) on its lower surface and zirconium oxide (ZrO_2) on its upper surface. For this end, the geometric of FG plates is taken as: h=0.0025 *m*, a=b=0.2 *m*. An identical value of Poisson's ratio v=0.3 is assumed for both ceramic and metal. The validation of the proposed refined hyperbolic plate model is carried out by comparing the obtained results with those computed via second order shear deformation plate theory (SSDT) developed by Shahrjerdi *et al.* (2011) and the higher-order shear deformation plate theory (HSDT) developed by Huang and Shen (2004).

As clearly shown in Table 4, the results of the (SSDT)

Table 5 Non-dimensional natural frequency parameter of simply supported (Si_3N_4/SUS304) FG plate in thermal environments

Mode (1,1) Natural frequency of (Si_3N_4/SUS304) FG plate		T_b=300(K)				
			T_t=400(K)		T_t=600(K)	
		T_t=300(K)	Temperature dependent	Temperature independent	Temperature dependent	Temperature independent
Si_3N_4	SSDT(a)	12.506	12.175	12.248	11.461	11.716
	TSDT(b)	12.495	13.397	12.382	11.984	12.213
	Present	12.519	12.319	12.389	11.899	12.126
p=0.5	SSDT(a)	8.652	8.361	8.405	7.708	7.887
	TSDT(b)	8.675	8.615	8.641	8.269	8.425
	Present	8.617	8.461	8.507	8.127	8.281
p=1	SSDT(a)	7.584	7.306	7.342	6.674	6.834
	TSDT(b)	7.555	7.474	7.514	7.171	7.305
	Present	7.551	7.406	7.444	7.090	7.225
p=2	SSDT(a)	6.811	6.545	6.575	5.929	6.077
	TSDT(b)	6.777	6.693	6.728	6.398	6.523
	Present	6.777	6.638	6.670	6.330	6.454
SUS304	SSDT(a)	5.410	5.161	5.178	4.526	4.682
	TSDT(b)	5.405	5.311	5.335	4.971	5.104
	Present	5.415	5.278	5.300	4.929	5.061

[a] Shahrjerdi *et al*. (2011) [b] Huang and Shen (2004)

Table 6 Non-dimensional frequency parameter of simply supported (ZrO_2/Ti-6Al-4V) FG plate in thermal environments (*p*=2)

Mode numbers of of (ZrO_2/Ti-6Al-4V) FG plate		T_b=300(K)				
			T_t=400(K)		T_t=600(K)	
		T_t=300(K)	Temperature dependent	Temperature independent	Temperature dependent	Temperature independent
(1,1)	SSDT(a)	6.333	5.992	6.132	5.139	5.711
	TSDT(b)	6.286	6.101	6.238	5.612	6.056
	Present	6.294	6.055	6.189	5.476	5.974
(1,2)	SSDT(a)	14.896	14.383	14.684	13.260	14.253
	TSDT(b)	14.625	14.372	14.655	13.611	14.474
	Present	14.699	14.301	14.588	13.453	14.363
(2,2)	SSDT(a)	22.608	21.942	22.386	20.557	21.935
	TSDT(b)	21.978	21.653	22.078	20.652	21.896
	Present	22.197	21.663	22.082	20.581	21.849
(1,3)	SSDT(a)	27.392	26.630	27.163	25.077	26.700
	TSDT(b)	26.454	26.113	26.605	24.961	26.435
	Present	26.811	26.190	26.689	24.954	26.446
(2,3)	SSDT(a)	34.106	33.211	33.867	31.425	33.384
	TSDT(b)	32.659	32.239	32.840	30.904	32.664
	Present	33.271	32.540	33.148	31.118	32.904

[a] Shahrjerdi *et al*. (2011) [b] Huang and Shen (2004)

plate theory developed by Shahrjerdi *et al.* (2011) and the (HSDT) plate theory developed by Huang and Shen (2004) are in a good agreement with the present results of refined hyperbolic plate theory (RSDT) and these for all values of power law index *p*, either for the case of temperature-dependent and temperature-independent FG plates. Also, inspection of Tables 4 reveals that the dimensionless fundamental frequencies of the FG plate decreases with the increase of power law index *p* and the temperature rise decreases the dimensionless fundamental frequencies.

Example 3

In the third example, a FG (Si_3N_4/SUS304) plate is examined. For this materials, the Poisson's ratio is taken *v*=0.28. The dimensionless fundamental frequencies obtained by present refined hyperbolic plate theory (RSDT) are compared with the published results of Shahrjerdi *et al.* (2011) and Huang and Shen (2004) in Table 5 for different values of power law index *p*. It can be seen that the fundamental frequency values computed from present model are in a good agreement with those reported by Shahrjerdi *et al.* (2011) and Huang and Shen (2004).

Example 4

In the section, the comparison is performed for (ZrO_2/Ti-6Al-4V) FG plate. This example aims to verify the obtained results with (SSDT) of Shahrjerdi *et al*. (2011) and (HSDT) of Huang and Shen (2004). The non-dimensional fundamental frequency is given in Table 6 for different vibration mode. For the modes (*m*,*n*), the integers *m* and *n* denote the number of half-waves in the *x* and *y* directions, respectively. It is observed that the present refined hyperbolic plate theory is in a good agreement with the previously published results (Shahrjerdi *et al*. 2011, Huang and Shen 2004) and these for different considered shape mode.

Example 5

In order to verify the accuracy of the present theory for large value of volume fraction index *p* and different values of thermal loads, an (Si_3N_4/SUS304) FG plate is now examined. The non-dimensional frequencies for FG (Si_3N_4/SUS304) plates predicted by Shahrjerdi *et al*. (2011) using second order shear deformation theory (SSDT), and present theory are presented in Table 7. An excellent agreement between the results predicted by (SSDT) of Shahrjerdi *et al*. (2011) and present theory is observed. It should be noted that the present theory contains four unknowns as against seven in the case of (SSDT) of Shahrjerdi *et al*. (2011). It can be concluded that the present theory is not only accurate but also efficient and simple in predicting the free vibration responses of FG plates in thermal environment.

4.2.2 Numerical results of present study

In the view of previous sections, it is can be seen that the proposed theory delivers results which are in good agreement with second order shear deformation plate theory (SSDT) developed by Shahrjerdi *et al.* (2011) and the higher-order shear deformation plate theory (HSDT) developed by Huang and Shen (2004) of the vibrated FG plate in thermal environment. In this example, the effects different parameters such as the power law index *p*, the mode numbers, and temperature fields on the free vibration

Table 7 Non-dimensional natural frequency of temperature dependent (Si_3N_4/SUS304) FG plate for different volume fraction index p in thermal environments Mode (1, 1)

Thermal Loads T_0 = 300 (K), b = a = 0.2, h = 0.025		T_b=300(K) T_t=300(K)	T_b=300(K) T_t=300(K)	T_b=300(K) T_t=300(K)
Si_3N_4	SSDT(a)	12.506	12.175	11.461
	Present	12.519	12.319	11.899
P=0.5	SSDT(a)	8.652	8.361	7.708
	Present	8.617	8.461	8.127
p=10	SSDT(a)	5.907	5.645	5.031
	Present	5.868	5.731	5.412
p=20	SSDT(a)	5.711	5.450	4.825
	Present	5.676	5.540	5.210
p=40	SSDT(a)	5.591	5.329	4.694
	Present	5.558	5.420	5.083
SUS304	SSDT(a)	5.410	5.161	4.526
	Present	5.415	5.278	4.929

(a) Shahrjerdi *et al*. (2011)

responses of FG plates are investigated here. All predicted results are carried out using present refined hyperbolic plate theory (RSDT).

Table 8 shows the non-dimensional frequencies values in (ZrO_2/Ti-6Al-4V) FG plate for different thermal loads. The non-dimensional natural frequency parameter is defined as $\overline{\omega} = \omega\left(a^2/h\right)\sqrt{\rho_b\left(1-\nu^2\right)/E_b}$, where E_b and ρ_b are at T_0=300(K) (Shahrjerdi *et al*. 2011). To see the effect of the power index p on the frequencies, the same values of the thermal load and the shape mode are considered. It is observed that the result for plates is in between those for pure material plates, because Young's modulus increases from pure metal to pure ceramic. Also, the frequencies decrease by increasing the temperature difference between top and bottom surfaces for the same value of power law index and shape mode that represent the effects of thermal loads. The difference between temperature-dependent and independent FG plates is less significant, Table 7 reveals the smaller frequencies in temperature-dependent FG plates, which proves the accuracy and effectiveness of temperature-dependent material properties.

The variation of the first four frequencies as a function of uniform, linear, nonlinear and sinusoidal temperature fields in simply supported FG plate is plotted in Figs. 6-8. The combination of (ZrO_2/Ti-6Al-4V) (Table 3) is assumed with material and geometric parameters of p=1, a=b=0.2 and a=h=10. The non-dimensional natural frequency parameter is defined as $\overline{\omega} = \omega\left(b^2/\pi^2\right)\sqrt{I_0/D_0}$, where $I_0 = \rho h$ and $D_0 = Eh^3/12\left(1-\nu^2\right)$ and it is noted that ρ, ν and E are chosen to be the values of (ZrO_2/Ti-6Al-4V) evaluated at the room temperature. As expected, the frequencies are reduced with increasing temperature and this is due to the decrease of Young's modulus with rising temperatures. It can be seen that the decreasing slope of frequencies in lower modes is smaller than those in higher modes. At the same temperature, we note that the difference between two consecutive lower modes is greater than that in two consecutive higher modes.

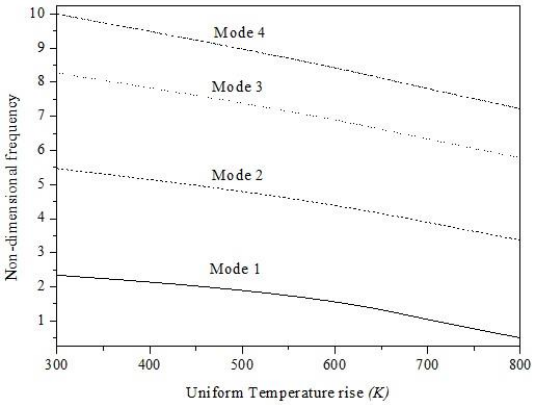

Fig. 6 First four non-dimensional frequency parameters versus uniform temperature field for simply supported (ZrO_2/Ti-6Al-4V) FG plate (a/h=10, a=0.2, p=1)

Table 8 Non-dimensional natural frequency parameter of simply supported (ZrO_2/Ti-6Al-4V) FG plate in thermal environments and for different modes of vibration

Mode numbers of FGP ZrO_2/Ti-6Al-4V)		T_b=300(K)				
		T_t=300(K)	T_t=400(K)		T_t=600(K)	
			Temperature dependent	Temperature independent	Temperature dependent	Temperature independent
ZrO_2	(1,1)	8.288	7.818	8.070	6.547	7.613
	(1,2)	19.388	18.623	19.157	16.895	18.686
	(2,2)	29.312	28.285	29.072	26.125	28.586
	(1,3)	35.427	34.231	35.176	31.779	34.669
	(2,3)	43.996	42.579	43.742	39.766	43.229
p=0.5	(1,1)	7.120	6.791	6.968	5.941	6.656
	(1,2)	16.668	16.131	16.509	14.945	16.185
	(2,2)	25.217	24.498	25.051	23.0b09	24.717
	(1,3)	30.488	29.654	30.315	27.960	29.966
	(2,3)	37.881	36.896	37.706	34.954	37.355
p=1	(1,1)	6.665	6.383	6.537	5.675	6.275
	(1,2)	15.593	15.131	15.458	14.125	15.185
	(2,2)	23.579	22.961	23.440	21.691	23.158
	(1,3)	28.501	27.784	28.355	26.337	28.061
	(2,3)	35.402	34.557	35.255	32.896	34.958
p=2	(1,1)	6.294	6.055	6.189	5.476	5.974
	(1,2)	14.699	14.301	14.588	13.453	14.363
	(2,2)	22.197	21.663	22.082	20.581	21.849
	(1,3)	26.811	26.190	26.689	24.954	26.446
	(2,3)	33.271	32.540	33.148	31.118	32.904
Ti-6Al-4V	(1,1)	5.410	5.290	5.357	5.097	5.250
	(1,2)	12.654	12.435	12.598	12.034	12.485
	(2,2)	19.132	18.823	19.073	18.239	18.956
	(1,3)	23.122	22.757	28.654	22.060	22.939
	(2,3)	28.716	28.274	28.654	27.420	28.530

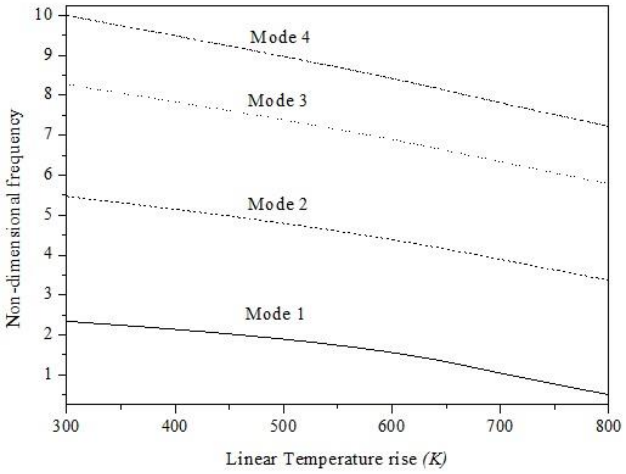

Fig. 7 First four non-dimensional frequency parameters versus linear temperature field for simply supported (ZrO_2/Ti-6Al-4V) FG plate (a/h=10, a=0.2, p=1)

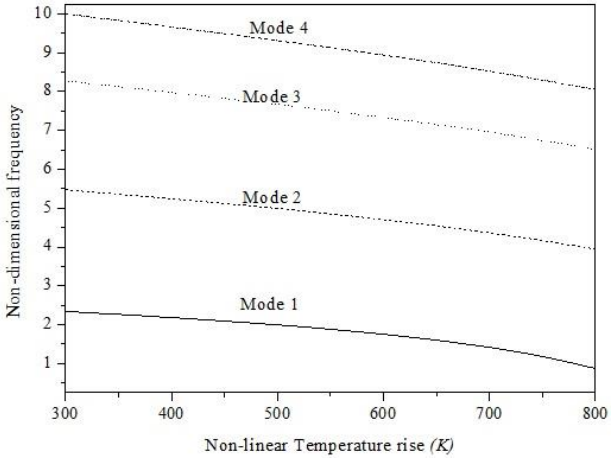

Fig. 8 First four non-dimensional frequency parameters versus nonlinear temperature field for simply supported (ZrO_2/Ti-6Al-4V) FG plate (a/h=10, a=0.2, p=1)

5. Conclusions

A novel hyperbolic shear deformation plate theory is developed for temperature-dependent free vibration of FG plates subjected to uniform, linear, nonlinear, and sinusoidal temperature fields is presented. Material properties of FG plates are assumed to be temperature-dependent and graded through the thickness according to a power-law distribution in terms of volume fractions of constituents. By considering further simplifying suppositions to the existing higher order shear deformation theory, with incorporation of an undetermined integral term, the present theory has only four unknowns, which is even less than the other shear deformation theories, and hence, make this model simple and efficient to employ. The equation of motion of the vibrated structure obtained via the classical Hamilton's principle and solved using Navier's steps. The subsequent main points can be drawn from the present study:

(1) The accuracy of the present work is ascertained by comparing it with existing shear deformation theory (HSDT) and excellent agreement was observed.

(2) The frequency decreases as temperature change increases in all types of temperature fields.

(3) The present novel hyperbolic shear deformation plate theory is not only accurate but also simple in predicting the vibration analysis of FG plates in thermal environment.

Finally, the formulation lend sit self particularly well to study several problems related to the hygro-thermomechanical deformation of laminated and FG structures (Bouderba *et al.* 2016, Beldjelili *et al.* 2016, Bousahla *et al.* 2016), also by using the nonlocal strain gradient model for analysis of mechanical behaviour of nanostructures reinforced with nanoparticles and carbon nanotubes (Bessaim *et al.* 2015, Kolahchi and Bidgoli 2016, Arani and Kolahchi 2016, Zamanian *et al.* 2017, Shokravi 2017, Hajmohammad *et al.* 2018, Amnieh *et al.* 2018, Karami *et al.* 2018), which will be considered in the near future. The present computations also provide a solid benchmark for verification of finite element and other numerical simulations of FGM nanobeam mechanics.

References

Abualnour, M., Houari, M.S.A., Tounsi, A., Adda Bedia, E.A. and Mahmoud, S.R. (2018), "A novel quasi-3D trigonometric plate theory for free vibration analysis of advanced composite plates", *Compos. Struct.*, **184**, 688-697.

Ahmed, A. (2014), "Post buckling analysis of sandwich beams with functionally graded faces using a consistent higher order theory", *Int. J. Civil Struct. Environ.*, **4**(2), 59-64.

Abdelaziz, H.H., Meziane, M.A.A., Bousahla, A.A., Tounsi, A., Mahmoud, S.R. and Alwabli, A.S. (2017), "An efficient hyperbolic shear deformation theory for bending, buckling and free vibration of FGM sandwich plates with various boundary conditions", *Steel Compos. Struct.*, **25**(6), 693-704.

Akbaş, Ş.D. (2015), "Wave propagation of a functionally graded beam in thermal environments", *Steel Compos. Struct.*, **19**(6), 1421-1447.

Alijani, F., Bakhtiari-Nejad, F. and Amabili, M. (2011), "Nonlinear vibrations of FGM rectangular plates in thermal environments", *Nonlin. Dyn.*, **66**(3), 251-270.

Allahverdizadeh, A., Naei, M.H. and Bahrami, M.N. (2008), "Nonlinear free and forced vibration analysis of thin circular functionally graded plates", *J. Sound Vibr.*, **310**(4), 966-984.

Amnieh, H.B., Zamzam, M.S. and Kolahchi, R. (2018), "Dynamic analysis of non-homogeneous concrete blocks mixed by SiO2 nanoparticles subjected to blast load experimentally and theoretically", *Constr. Build. Mater.*, **174**, 633-644.

Arani, A.G., Cheraghbak, A. and Kolahchi, R. (2016), "Dynamic buckling of FGM viscoelastic nano-plates resting on orthotropic elastic medium based on sinusoidal shear deformation theory", *Struct. Eng. Mech.*, **60**(3), 489-505.

Arani, A.J. and Kolahchi, R. (2016), "Buckling analysis of embedded concrete columns armed with carbon nanotubes", *Comput. Concrete*, **17**(5), 567-578.

Attia, A., Tounsi, A., Bedia, E.A. and Mahmoud, S.R. (2015), "Free vibration analysis of functionally graded plates with temperature-dependent properties using various four variable refined plate theories", *Steel Compos. Struct.*, **18**(1), 187-212.

Behravan Rad, A. (2015), "Thermo-elastic analysis of functionally graded circular plates resting on a gradient hybrid foundation", *Appl. Math. Comput.*, **256**, 276-298.

Belabed, Z., Houari, M.S.A., Tounsi, A., Mahmoud, S.R. and Bég, O.A. (2014), "An efficient and simple higher order shear and

normal deformation theory for functionally graded material (FGM) plates", *Compos. Part B*: *Eng*., **60**, 274-283.
Belabed, Z., Bousahla, A.A., Houari, M.S.A., Tounsi, A. and Mahmoud, S.R. (2018), "A new 3-unknown hyperbolic shear deformation theory for vibration of functionally graded sandwich plate", *Earthq. Struct*., **14**(2), 103-115.
Beldjelili, Y., Tounsi, A. and Mahmoud, S.R. (2016), "Hygro-thermo-mechanical bending of S-FGM plates resting on variable elastic foundations using a four-variable trigonometric plate theory", *Smart Struct. Syst*., **18**(4), 755-786.
Benahmed, A., Houari, M.S.A., Benyoucef, S., Belakhdar, K. and Tounsi, A. (2017), "A novel quasi-3D hyperbolic shear deformation theory for functionally graded thick rectangular plates on elastic foundation", *Geomech. Eng*., **12**(1), 9-34.
Bessaim, A., Houari, M.S.A., Bernard, F. and Tounsi, A. (2015), "A nonlocal quasi-3D trigonometric plate model for free vibration behaviour of micro/nanoscale plates", *Struct. Eng. Mech*., **56**(2), 223-240.
Besseghier, A., Houari, M.S.A., Tounsi, A. and Mahmoud, S.R. (2017), "Free vibration analysis of embedded nanosize FG plates using a new nonlocal trigonometric shear deformation theory", *Smart Struct. Syst*., **19**(6), 601-614.
Bouderba, B., Houari, M.S.A., Tounsi, A. and Mahmoud, S.R. (2016), "Thermal stability of functionally graded sandwich plates using a simple shear deformation theory", *Struct. Eng. Mech*., **58**(3), 397-422.
Bousahla, A.A., Benyoucef, S., Tounsi, A. and Mahmoud, S.R. (2016), "On thermal stability of plates with functionally graded coefficient of thermal expansion", *Struct. Eng. Mech*., **60**(2), 313-335.
Chakraverty, S. and Pradhan, K.K. (2014), "Free vibration of exponential functionally graded rectangular plates in thermal environment with general boundary conditions", *Aerosp. Sci. Technol*., **36**, 132-156.
Chikh, A., Tounsi, A., Hebali, H. and Mahmoud, S.R. (2017), "Thermal buckling analysis of cross-ply laminated plates using a simplified HSDT", *Smart Struct. Syst*., **19**(3), 289-297.
Cui, D. and Hu, H. (2016), "Thermal buckling and natural vibration of a rectangular thin plate with in-plane stick-slip-stop boundaries", *J. Vibr. Contr*., **22**(7), 1950-1966.
Darilmaz, K. (2015), "Vibration analysis of functionally graded material (FGM) grid systems", *Steel Compos. Struct*., **18**(2), 395-408.
Darilmaz, K., Aksoylu, M.G. and Durgun, Y. (2015), "Buckling analysis of functionally graded material grid systems", *Struct. Eng. Mech*., **54**(5), 877-890.
Dinh Duc, N. and Hong Cong, P. (2015), "Nonlinear vibration of thick FGM plates on elastic foundation subjected to thermal and mechanical loads using the first-order shear deformation plate theory", *Cogent Eng*., **2**(1), 1045222.
Ebrahimi, F. (2013), "Analytical investigation on vibrations and dynamic response of functionally graded plate integrated with piezoelectric layers in thermal environment", *Mech. Adv. Mater. Struct*., **20**(10), 854-870.
Ebrahimi, F. and Dashti, S. (2015), "Free vibration analysis of a rotating non-uniform functionally graded beam", *Steel Compos. Struct*., **19**(5), 1279-1298.
Ebrahimi, F. and Habibi, S. (2016), "Deflection and vibration analysis of higher-order shear deformable compositionally graded porous plate", *Steel Compos. Struct*., **20**(1), 205-225.
Ebrahimi, F. and Jafari, A. (2016), "Thermo-mechanical vibration analysis of temperature-dependent porous FG beams based on Timoshenko beam theory", *Struct. Eng. Mech*., **59**(2), 343-371.
El-Haina, F., Bakora, A., Bousahla, A.A., Tounsi, A. and Mahmoud, S.R. (2017), "A simple analytical approach for thermal buckling of thick functionally graded sandwich plates", *Struct. Eng. Mech*., **63**(5), 585-595.
Ferreira, A.J.M., Castro, L.M. and Bertoluzza, S. (2009), "A high order collocation method for the static and vibration analysis of composite plates using a first-order theory", *Compos. Struct*., **89**(3), 424-432.
Hachemi, H., Kaci, A., Houari, M.S.A., Bourada, M., Tounsi, A. and Mahmoud, S.R. (2017), "A new simple three-unknown shear deformation theory for bending analysis of FG plates resting on elastic foundations", *Steel Compos. Struct*., **25**(6), 717-726.
Hajmohammad, M.H., Zarei, M.S., Nouri, A. and Kolahchi, R. (2017), "Dynamic buckling of sensor/functionally graded-carbon nanotube-reinforced laminated plates/actuator based on sinusoidal-visco-piezoelasticity theories", *J. Sandw. Struct. Mater*., 1099636217720373.
Hajmohammad, M.H., Maleki, M. and Kolahchi, R. (2018), "Seismic response of underwater concrete pipes conveying fluid covered with nano-fiber reinforced polymer layer", *Soil Dyn. Earthq. Eng*., **110**, 18-27.
Hirwani, C.K., Panda, S.K., Mahapatra, T.R. and Mahapatra, S.S. (2017), "Numerical study and experimental validation of dynamic characteristics of delaminated composite flat and curved shallow shell structure", *J. Aerosp. Eng*., **30**(5), 04017045.
Hirwani, C.K. and Panda, S.K. (2018), "Numerical nonlinear frequency analysis of pre-damaged curved layered composite structure using higher-order finite element method", *Int. J. Non-Lin. Mech*., **102**, 14-24.
Hirwani, C.K., Panda, S.K. and Mahapatra, T.R. (2018a), "Thermomechanical deflection and stress responses of delaminated shallow shell structure using higher-order theories", *Compos. Struct*., **184**, 135-145.
Hirwani, C.K., Panda, S.K. and Mahapatra, T.R. (2018b), "Nonlinear finite element analysis of transient behavior of delaminated composite plate", *J. Vibr. Acoust*., **140**(2), 021001.
Hirwani, C.K., Biswash, S., Mehar, K. and Panda, S.K. (2018c), "Numerical flexural strength analysis of thermally stressed delaminated composite structure under sinusoidal loading", In IOP Conference Series: Materials Science and Engineering, **22**(1), 012019.
Houari, M.S.A., Tounsi, A. and Bég, O.A. (2013), "Thermoelastic bending analysis of functionally graded sandwich plates using a new higher order shear and normal deformation theory", *Int. J. Mech. Sci*., **76**, 102-111.
Houari, M.S.A., Tounsi, A., Bessaim, A. and Mahmoud, S.R. (2016), "A new simple three-unknown sinusoidal shear deformation theory for functionally graded plates", *Steel Compos. Struct*., **22**(2), 257-276.
Huang, X.L. and Shen, H.S. (2004), "Nonlinear vibration and dynamic response of functionally graded plates in thermal environments", *Int. J. Sol. Struct*., **41**(9), 2403-2427.
Joshi, P.V., Jain, N.K., Ramtekkar, G.D. and Virdi, G.S. (2016), "Vibration and buckling analysis of partially cracked thin orthotropic rectangular plates in thermal environment", *Thin-Wall. Struct*., **109**, 143-158.
Joshi, P.V., Gupta, A., Jain, N.K., Salhotra, R., Rawani, A.M. and Ramtekkar, G.D. (2017), "Effect of thermal environment on free vibration and buckling of partially cracked isotropic and FGM micro plates based on a non-classical Kirchhoff's plate theory: An analytical approach", *Int. J. Mech. Sci*., **131**, 155-170.
Kaci, A., Houari, M.S.A., Bousahla, A.A., Tounsi, A. and Mahmoud, S.R. (2018), "Post-buckling analysis of shear-deformable composite beams using a novel simple two-unknown beam theory", *Sturct. Eng. Mech*., **65**(5), 621-631.
Kar, V.R. and Panda, S.K. (2014), "Large deformation bending analysis of functionally graded spherical shell using FEM", *Struct. Eng. Mech*., **53**(4), 661-679.
Kar, V.R. and Panda, S.K. (2015a), "Nonlinear flexural vibration

of shear deformable functionally graded spherical shell panel", *Steel Compos. Struct.*, **18**(3), 693-709.

Kar, V.R. and Panda, S.K. (2015b), "Free vibration responses of temperature dependent functionally graded curved panels under thermal environment", *Lat. Am. J. Sol. Struct.*, **12**(11), 2006-2024.

Kar, V.R., Mahapatra, T.R. and Panda, S.K. (2017), "Effect of different temperature load on thermal postbuckling behaviour of functionally graded shallow curved shell panels", *Compos. Struct.*, **160**, 1236-1247.

Karami, B., Janghorban, M. and Tounsi, A. (2018), "Nonlocal strain gradient 3D elasticity theory for anisotropic spherical nanoparticles", *Steel Compos. Struct.*, **27**(2), 201-216.

Karami, B., Janghorban, M. and Tounsi, A. (2018), "Variational approach for wave dispersion in anisotropic doubly-curved nanoshells based on a new nonlocal strain gradient higher order shell theory", *Thin-Wall. Struct.*, **129**, 251-264.

Kant, T. (1993), "A critical review and some results of recently developed refined theories of fiber-reinforced laminated composites and sandwiches", *Compos. Struct.*, **23**(4), 293-312.

Kant, T. and Swaminathan, K. (2001), "Free vibration of isotropic, orthotropic, and multilayer plates based on higher order refined theories", *J. Sound Vibr.*, **241**(2), 319-327.

Khetir, H., Bachir Bouiadjra, M., Houari, M.S.A., Tounsi, A. and Mahmoud, S.R. (2017), "A new nonlocal trigonometric shear deformation theory for thermal buckling analysis of embedded nanosize FG plates", *Struct. Eng. Mech.*, **64**(4), 391-402.

Kim, Y.W. (2005), "Temperature dependent vibration analysis of functionally graded rectangular plates", *J. Sound Vibr.*, **284**(3), 531-549.

Kirchhoff, G.R. (1850), *Uber Das Gleichgewicht Und Die Bewegung Einer Elastischen Scheibe*.

Kolahchi, R., Safari, M. and Esmailpour, M. (2016a), "Dynamic stability analysis of temperature-dependent functionally graded CNT-reinforced visco-plates resting on orthotropic elastomeric medium", *Compos. Struct.*, **150**, 255-265.

Kolahchi, R. and Bidgoli, A.M. (2016), "Size-dependent sinusoidal beam model for dynamic instability of single-walled carbon nanotubes", *Appl. Math. Mech.*, **37**(2), 265-274.

Kolahchi, R., Zarei, M.S., Hajmohammad, M.H. and Nouri, A. (2017a), "Wave propagation of embedded viscoelastic FG-CNT-reinforced sandwich plates integrated with sensor and actuator based on refined zigzag theory", *Int. J. Mech. Sci.*, **130**, 534-545.

Kolahchi, R., Zarei, M.S., Hajmohammad, M.H. and Oskouei, A.N. (2017b), "Visco-nonlocal-refined zigzag theories for dynamic buckling of laminated nanoplates using differential cubature-Bolotin methods", *Thin-Wall. Struct.*, **113**, 162-169.

Lei, Z.X., Liew, K.M. and Yu, J.L. (2013), "Free vibration analysis of functionally graded carbon nanotube-reinforced composite plates using the element-free kp-Ritz method in thermal environment", *Compos. Struct.*, **106**, 128-138.

Li, Q., Iu, V.P. and Kou, K.P. (2008), "Three-dimensional vibration analysis of functionally graded material sandwich plates", *J. Sound Vibr.*, **311**(1), 498-515.

Li, Q., Iu, V.P. and Kou, K.P. (2009), "Three-dimensional vibration analysis of functionally graded material plates in thermal environment", *J. Sound Vibr.*, **324**(3), 733-750.

Li, S.R. and Cheng, C.J. (2009), "Free vibration of functionally graded material beams with surface-bonded piezoelectric layers in thermal environment", *Appl. Math. Mech.*, **30**(8), 969-982.

Lim, C.W., Yang, Q. and Lü, C.F. (2009), "Two-dimensional elasticity solutions for temperature-dependent in-plane vibration of FGM circular arches", *Compos. Struct.*, **90**(3), 323-329.

Lim, T.K. and Kim, J.H. (2017), "Thermo-micromechanical vibration behaviors of FGM structures with neutral surface", *Appl. Mech. Mater.*, **864**, 162-166.

Madani, H., Hosseini, H. and Shokravi, M. (2016), "Differential cubature method for vibration analysis of embedded FG-CNT-reinforced piezoelectric cylindrical shells subjected to uniform and non-uniform temperature distributions", *Steel Compos. Struct.*, **22**(4), 889-913.

Mahapatra, T.R. and Panda, S.K. (2015), "Thermoelastic vibration analysis of laminated doubly curved shallow panels using non-linear FEM", *J. Therm. Stress.*, **38**(1), 39-68.

Mahapatra, T.R., Kar, V.R. and Panda, S.K. (2015), "Nonlinear free vibration analysis of laminated composite doubly curved shell panel in hygrothermal environment", *J. Sandw. Struct. Mater.*, **17**(5), 511-545.

Mahapatra, T.R. and Panda, S.K. (2016), "Nonlinear free vibration analysis of laminated composite spherical shell panel under elevated hygrothermal environment: A micromechanical approach", *Aerosp. Sci. Technol.*, **49**, 276-288.

Mahapatra, T.R., Kar, V.R. and Panda, S.K. (2016a), "Large amplitude vibration analysis of laminated composite spherical panels under hygrothermal environment", *Int. J. Struct. Stab. Dyn.*, **16**(3), 1450105.

Mahapatra, T.R., Panda, S.K. and Kar, V.R. (2016b), "Nonlinear hygro-thermo-elastic vibration analysis of doubly curved composite shell panel using finite element micromechanical model", *Mech. Adv. Mater. Struct.*, **23**(11), 1343-1359.

Mahapatra, T.R., Panda, S.K. and Kar, V.R. (2016c), "Nonlinear flexural analysis of laminated composite panel under hygro-thermo-mechanical loading-a micromechanical approach", *Int. J. Comput. Meth.*, **13**(3), 1650015.

Mahapatra, T.R., Kar, V.R., Panda, S.K. and Mehar, K. (2017), "Nonlinear thermoelastic deflection of temperature-dependent FGM curved shallow shell under nonlinear thermal loading", *J. Therm. Stress.*, **40**(9), 1184-1199.

Mahi, A., Adda Bedia, E.A. and Tounsi, A. (2015), "A new hyperbolic shear deformation theory for bending and free vibration analysis of isotropic, functionally graded, sandwich and laminated composite plates", *Appl. Math. Model.*, **39**, 2489-2508.

Malekzadeh, P., Shahpari, S.A. and Ziaee, H.R. (2010), "Three-dimensional free vibration of thick functionally graded annular plates in thermal environment", *J. Sound Vibr.*, **329**(4), 425-442.

Malekzadeh, P. and Heydarpour, Y. (2012), "Free vibration analysis of rotating functionally graded cylindrical shells in thermal environment", *Compos. Struct.*, **94**(9), 2971-2981.

Malekzadeh, P. and Monajjemzadeh, S.M. (2016), "Dynamic response of functionally graded beams in a thermal environment under a moving load", *Mech. Adv. Mater. Struct.*, **23**(3), 248-258.

Mehar, K., Panda, S.K., Dehengia, A. and Kar, V.R. (2016), "Vibration analysis of functionally graded carbon nanotube reinforced composite plate in thermal environment", *J. Sandw. Struct. Mater.*, **18**(2), 151-173.

Mehar, K., Panda, S.K. and Mahapatra, T.R. (2017a), "Thermoelastic nonlinear frequency analysis of CNT reinforced functionally graded sandwich structure", *Eur. J. Mech.-A/Sol.*, **65**, 384-396.

Mehar, K., Panda, S.K., Bui, T.Q. and Mahapatra, T.R. (2017b), "Nonlinear thermoelastic frequency analysis of functionally graded CNT-reinforced single/doubly curved shallow shell panels by FEM", *J. Therm. Stress.*, **40**(7), 899-916.

Menasria, A., Bouhadra, A., Tounsi, A., Bousahla, A.A. and Mahmoud, S.R. (2017), "A new and simple HSDT for thermal stability analysis of FG sandwich plates", *Steel Compos. Struct.*, **25**(2), 157-175.

Mouffoki, A., Adda Bedia, E.A., Houari, M.S.A., Tounsi, A. and Mahmoud, S.R. (2017), "Vibration analysis of nonlocal advanced nanobeams in hygro-thermal environment using a new two-unknown trigonometric shear deformation beam

theory", *Smart Struct. Syst.*, **20**(3), 369-383.
Nguyen, T.K. (2015), "A higher-order hyperbolic shear deformation plate model for analysis of functionally graded materials", *Int. J. Mech. Mater. Des.*, **11**(2), 203-219.
Panda, S.K. and Mahapatra, T.R. (2014), "Nonlinear finite element analysis of laminated composite spherical shell vibration under uniform thermal loading", *Meccan.*, **49**(1), 191-213.
Pandey, S. and Pradyumna, S. (2015), "Free vibration of functionally graded sandwich plates in thermal environment using a layerwise theory", *Eur. J. Mech.-A/Sol.*, **51**, 55-66.
Parandvar, H. and Farid, M. (2016), "Nonlinear dynamic response of functionally graded shallow shells under harmonic excitation in thermal environment using finite element method", *Compos. Struct.*, **149**, 351-361.
Praveen, G.N. and Reddy, J.N. (1998), "Nonlinear transient thermoelastic analysis of functionally graded ceramic-metal plates", *Int. J. Sol. Struct.*, **35**(33), 4457-4476.
Reddy, J.N. (1984), "A simple higher-order theory for laminated composite plates", *J. Appl. Mech.*, **51**(4), 745-752.
Reissner, E. (1945), "The effect of transverse shear deformation on the bending of elastic plates".
Sahoo, S.S., Panda, S.K. and Mahapatra, T.R. (2016), "Static, free vibration and transient response of laminated composite curved shallow panel-an experimental approach", *Eur. J. Mech.-A/Sol.*, **59**, 95-113.
Sahoo, S.S., Hirwani, C.K., Panda, S.K. and Sen, D. (2017), "Numerical analysis of vibration and transient behaviour of laminated composite curved shallow shell structure: An experimental validation", *Sci. Iran.*
Shahrjerdi, A., Mustapha, F., Bayat, M. and Majid, D.L.A. (2011), "Free vibration analysis of solar functionally graded plates with temperature-dependent material properties using second order shear deformation theory", *J. Mech. Sci. Techol.*, **25**(9), 2195-2209.
Shi, G. (2007), "A new simple third-order shear deformation theory of plates", *Int. J. Sol. Struct.*, **44**(13), 4399-4417.
Setoodeh, A.R., Ghorbanzadeh, M. and Malekzadeh, P. (2012), "A two-dimensional free vibration analysis of functionally graded sandwich beams under thermal environment", *J. Mech. Eng. Sci.*, **226**(12), 2860-2873.
Shokravi, M. (2017), "Buckling of sandwich plates with FG-CNT-reinforced layers resting on orthotropic elastic medium using Reddy plate theory", *Steel Compos. Struct.*, **23**(6), 623-631.
Srinivas, S., Rao, C.J. and Rao, A.K. (1970), "An exact analysis for vibration of simply-supported homogeneous and laminated thick rectangular plates", *J. Sound Vibr.*, **12**(2), 187-199.
Sofiyev, A.H. and Kuruoglu, N. (2015), "Buckling of non-homogeneous orthotropic conical shells subjected to combined load", *Steel Compos. Struct.*, **19**(1), 1-19.
Sofiyev, A.H. and Osmancelebioglu, E. (2017), "The free vibration of sandwich truncated conical shells containing functionally graded layers within the shear deformation theory", *Compos. Part B: Eng.*, **120**, 197-211.
Sundararajan, N., Prakash, T. and Ganapathi, M. (2005), "Nonlinear free flexural vibrations of functionally graded rectangular and skew plates under thermal environments", *Fin. Elem. Analy. Des.*, **42**(2), 152-168.
Tounsi, A., Houari, M.S.A. and Bessaim, A. (2016), "A new 3-unknowns non-polynomial plate theory for buckling and vibration of functionally graded sandwich plate", *Struct. Eng. Mech.*, **60**(4), 547-565.
Wattanasakulpong, N., Prusty, G.B. and Kelly, D.W. (2013), "Free and forced vibration analysis using improved third-order shear deformation theory for functionally graded plates under high temperature loading", *J. Sandw. Struct. Mater.*, **15**(5), 583-606.
Woo, J., Meguid, S.A. and Ong, L.S. (2006), "Nonlinear free vibration behavior of functionally graded plates", *J. Sound Vibr.*, **289**(3), 595-611.
Wu, Z., Cheung, Y.K., Lo, S.H. and Chen, W. (2008), "Effects of higher-order global-local shear deformations on bending, vibration and buckling of multilayered plates", *Compos. Struct.*, **82**(2), 277-289.
Xiao, J.R., Batra, R.C., Gilhooley, D.F., Gillespie, J.W. and McCarthy, M.A. (2007), "Analysis of thick plates by using a higher-order shear and normal deformable plate theory and MLPG method with radial basis functions", *Comput. Meth. Appl. Mech. Eng.*, **196**(4), 979-987.
Yang, J. and Shen, H.S. (2002), "Vibration characteristics and transient response of shear-deformable functionally graded plates in thermal environments", *J. Sound Vibr.*, **255**(3), 579-602.
Yang, J. and Shen, H.S. (2003), "Nonlinear bending analysis of shear deformable functionally graded plates subjected to thermo-mechanical loads under various boundary conditions", *Compos. Part B: Eng.*, **34**(2), 103-115.
Yaghoobi, H., Valipour, M.S., Fereidoon, A. and Khoshnevisrad, P. (2014), "Analytical study on post buckling and nonlinear free vibration analysis of FG beams resting on nonlinear elastic foundation under thermo-mechanical loading using VIM", *Steel Compos. Struct.*, **17**(5), 753-776.
Younsi, A., Tounsi, A., Zaoui, F.Z., Bousahla, A.A. and Mahmoud, S.R. (2018), "Novel quasi-3D and 2D shear deformation theories for bending and free vibration analysis of FGM plates", *Geomech. Eng.*, **14**(6), 519-532.
Zamanian, M., Kolahchi, R. and Bidgoli, M.R. (2017), "Agglomeration effects on the buckling behaviour of embedded concrete columns reinforced with SiO2 nano-particles", *Wind Struct.*, **24**(1), 43-57.

CC

Appendix

The stiffness and inertia coefficients a_{ij} and M_{ij} appeared in governing Eq. (33) are as follows

$$
\begin{aligned}
a_{11} &= -\left(\alpha^2\left(A_{11}+A_{11}^T\right)+\beta^2\left(A_{22}^T+A_{66}\right)\right),\\
a_{12} &= -\alpha\beta\left(A_{12}+A_{66}\right),\\
a_{13} &= \alpha^3\left(B_{11}+B_{11}^T\right)+\alpha\beta^2\left(B_{12}+2B_{66}+B_{22}^T\right),\\
a_{14} &= \alpha\left(k_1B_{11}^s+k_2B_{12}^s-\left(k_1A^{'}+k_2B^{'}\right)B_{66}^s\beta^2\right)-k_1A^{'}\left(\alpha^3B_{11}^{sT}+\alpha\beta^2B_{22}^{sT}\right),\\
a_{22} &= -\left(\alpha^2\left(A_{66}+A_{11}^T\right)+\beta^2\left(A_{22}^T+A_{22}\right)\right),\\
a_{23} &= \beta^3\left(B_{11}+B_{11}^T\right)+\alpha^2\beta\left(B_{12}+2B_{66}+B_{22}^T\right)\\
a_{24} &= \beta\left(k_1B_{12}^s+k_2B_{22}^s-\left(k_1A^{'}+k_2B^{'}\right)B_{66}^s\alpha^2\right)-k_2B^{'}\left(\alpha^2\beta B_{11}^{sT}+\beta^3B_{22}^{sT}\right)\\
a_{33} &= -\left(\alpha^4\left(D_{11}+D_{11}^T\right)+2\alpha^2\beta^2(D_{12}+2D_{66})+\alpha^2\beta^2\left(D_{11}^T+D_{22}^T\right)+\beta^4\left(D_{22}+D_{22}^T\right)\right)\\
a_{34} &= -k_1\left(D_{11}^s\alpha^2+D_{12}^s\beta^2\right)+2(k_1A^{'}+k_2B^{'})D_{66}^s\alpha^2\beta^2-k_2\left(D_{22}^s\beta^2+D_{12}^s\alpha^2\right)+k_1A^{'}\alpha^4D_{11}^{sT}+k_2B^{'}\beta^4D_{22}^{sT}+(k_1A^{'}D_{22}^{sT}+k_2B^{'}D_{11}^{sT})\alpha^2\beta^2\\
a_{44} &= -k_1\left(\left(H_{11}^s+H_{11}^{sT}\right)k_1+H_{12}^sk_2\right)-k_1k_2\left(H_{11}^{sT}+H_{22}^{sT}\right)-(k_1A^{'}+k_2B^{'})^2H_{66}^s\alpha^2\beta^2\\
&\quad -k_2\left(H_{12}^sk_1+\left(H_{22}^s+H_{22}^{sT}\right)k_2\right)-\left(k_1A^{'}\right)^2A_{55}^s\alpha^2-\left(k_2B^{'}\right)^2A_{44}^s\beta^2
\end{aligned}
\tag{34}
$$

$$
\begin{aligned}
&M_{11}=-I_0,\ M_{13}=\alpha I_1,\ M_{14}=-k_1J_1A^{'}\alpha,\ M_{22}=-I_0,\\
&M_{23}=\beta I_1, M_{24}=-k_2B^{'}\beta J_1,\ M_{33}=-I_0-I_2(\alpha^2+\beta^2),\\
&M_{34}=J_2\left(k_1A^{'}\alpha^2+k_2B^{'}\beta^2\right),\ M_{44}=-K_2\left(\left(k_1A^{'}\right)^2\alpha^2+\left(k_2B^{'}\right)^2\beta^2\right)
\end{aligned}
$$